Preparation of Titanium Oxide Photocatalysts Anchored on Porous Silica Glass by a Metal Ion-Implantation Method and Their Photocatalytic Reactivities for the Degradation of 2-Propanol Diluted in Water

Hiromi Yamashita, Miwa Honda, Masaru Harada, Yuichi Ichihashi, and Masakazu Anpo*

Department of Applied Chemistry, Osaka Prefecture University, Gakuen-cho 1-1, Sakai, Osaka 599-8531, Japan

Takashi Hirao

Department of Electronic Engineering, Osaka University, Yamadaoka 1-1, Suita, Osaka 565-0871, Japan

Nobuhisa Itoh

Human Environment Systems Development Center, Matsushita Electric Industrial Company, Ltd., Seika-cho, Souraku, Kyoto 619-0237, Japan

Nobuya Iwamoto

Ion Engineering Research Institute Corporation, Tsuda-yamate, Hirakata, Osaka 573-0128, Japan

Received: June 30, 1998; In Final Form: September 25, 1998

Highly dispersed titanium oxide photocatalysts anchored onto transparent plates of porous silica glass were successfully prepared by metal ion implantation, and their photocatalytic reactivity for the liquid-phase photocatalytic degradation of an aqueous 2-propanol solution was compared with that in an aqueous TiO_2 dispersion. The titanium ions implanted into the porous silica glass are found to be present on the surface layer as isolated tetrahedral titanium oxide moieties by diffuse reflectance absorption, SIMS, XPS, and XAFS analyses. The specific photocatalytic reactivity of the anchored catalyst was much higher than that for TiO_2 powder, which may be attributed to the tetrahedrally coordinated titanium oxide moieties. Metal ion implantation is one of the novel and useful techniques to prepare highly efficient photocatalysts on glass plates.

Introduction

The design of highly efficient and selective photocatalytic systems which work in the reduction of global air and water pollution is of vital interest and one of the most desirable yet challenging goals in the research of environmentally friendly catalysts.[1,2] TiO_2 semiconductor photocatalysts are known as one of the most stable and highly reactive photocatalysts. The utilization of fine TiO_2 particles as photocatalysts has attracted a great deal of attention especially for such environmental applications.[2−5] Since the photocatalytic effectiveness strongly depends on the chemical and physical properties of the samples,[6,7] the design of a well-defined photocatalyst is indispensable not only for the development of efficient photocatalytic systems but also for an understanding of the stuctural bases of photocatalytic properties at the molecular level.

The photocatalytic degradation of various toxic compounds in aqueous solutions using irradiated small TiO_2 particle photocatalysts suspended in liquid solution has been widely studied. However, to avoid the filtration and suspension of small-particle photocatalysts, the design of efficient photocatalysts anchored on transparent supports or embedded onto/into transparent materials would be of greater significance.[8,9] Recently, the sol−gel method was used by several researchers to develop TiO_2-coated glasses and tiles, applying this photocatalyst for a practical way to maintain clean windows, to reduce the density of colonies of microorganisms, to eliminate offensive odors, and also to clean oil and other organic sheens on water.[10]

"Metal ion implantation" has been shown to be one of the most available procedures for enhancement of the electronic activities of semiconducting materials.[2,11,12] This technique was used to implant metal ions into various materials in a highly dispersed state. This advanced and unique process can be applied as a fascinating way to design active catalysts highly dispersed on various types of supports while clarifying the chemical nature of the active sites in order to develop efficient and useful photocatalytic systems.

In the present study, we deal with the preparation and characterization of highly active tetrahedral titanium oxide species implanted onto transparent porous silica glass by metal ion implantation and the successful utilization of these catalysts for the photocatalytic degradation of 2-propanol diluted in water.

Experimental Section

Titanium oxide catalysts anchored onto plates ($10 \times 8 \times 1$ mm, ~200 mg) of porous silica glass (PVG: Corning Code 7930, surface area 250 m^2/g) with various Ti contents were prepared by an advanced metal ion-implantation method using $TiCl_4$ as the source of Ti ions.[11,12] A systematic diagram of the ion implantation is shown in Figure 1. Ti ions produced in an ion chamber were accelerated by an electronic field and implanted into the target. The concentration of Ti ions in the

10.1021/jp982835q CCC: $15.00
Published on Web 12/05/1998

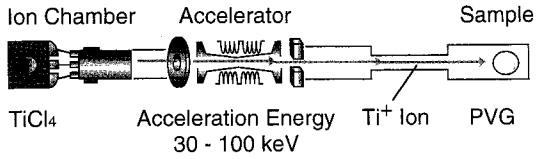

Figure 1. Systematic diagram of a metal ion (Ti^+) implantation.

ion beam was monitored by a mass analyzer. Acceleration at an energy level of 30−100 keV caused the implanted ions to replace the atoms on the surface layers of the silica glass. By variation of the duration of time for Ti ion implantation (0.5, 1, 2 h), the amount of Ti ions implanted into the surface regions of the silica glass could be controlled (4.3×10^{-7}, 8.7×10^{-7}, 17.3×10^{-7} mol/cat-g, respectively). The catalyst was heated in O_2 gas at 723 K for 5 h before use and then placed in a quartz cell with an aqueous solution of 2-propanol (2.6×10^{-3} mol/L, 25 mL), and the sample was irradiated at 295 K using UV light ($\lambda > 280$ nm) with a 100-W high-pressure Hg lamp under O_2 atmosphere in the system. The products were analyzed by gas chromatography. Specific photocatalytic reactivities were obtained by the normalization of the initial rates of 2-propanol conversion with the amounts of Ti ions included in the catalysts. An apparent quantum yield for the photocatalytic oxidative disappearance of 2-propanol was defined as the disappeared number of 2-propanol molecules relative to the number of adsorbed photons by standard potassium ferrioxalate chemical actinometry. A quantum yield described herein was the average of the repeated experiments, and an allowance of ca. ±10% was considered for error.

The diffuse reflectance absorption spectra were recorded with a Shimadzu UV 2200A spectrometer at 295 K. The X-ray photoelectron spectroscopy (XPS) spectra were measured at 295 K with a VG Scientific ESCASCOPE photoelectron spectrometer using Mg Kα radiation. The secondary ion mass spectroscopy (SIMS) spectra were measured with a Shimadzu/Kratos SIMS S1030. The X-ray absorption fine structure (XAFS) spectra, X-ray absorption near edge structure (XANES), and extended X-ray absorption fine structure (EXAFS) were measured at the BL-7C facility of the Photon Factory at the National Laboratory for High-Energy Physics, Tsukuba, Japan. The Ti K-edge absorption spectra were recorded in the fluorescence mode at 295 K. The normalized spectra were obtained by a procedure described in previous literature,[13] and Fourier transformation was performed on k^3-weighted EXAFS oscillations in the range 3−10 $Å^{-1}$. The curve-fitting of the EXAFS data was carried out by iterative nonlinear least-squares calculations, and the empirical backscattering parameter sets were extracted from the shell features of the titanium compounds.

Results and Discussion

UV irradiation of the titanium oxide catalyst anchored onto the porous silica glass plate prepared by advanced metal ion implantation (titanium oxide/PVG) in a diluted aqueous solution of 2-propanol under O_2 atmosphere led to the formation of acetone and CO_2. After prolonged UV irradiation, acetone was finally decomposed into CO_2. In the initial step, the yields of these photooxidative products increased linearly against the UV irradiation time, as shown in Figure 2. The formations of these products were detected neither under dark conditions nor under UV irradiation of porous silica glass in the absence of titanium oxides. The presence of titanium oxide anchored onto porous silica glass as well as UV irradiation is indispensable for the photocatalytic reaction to take place, and the degradation of 2-propanol occurs photocatalytically on the TiO_2 surface.

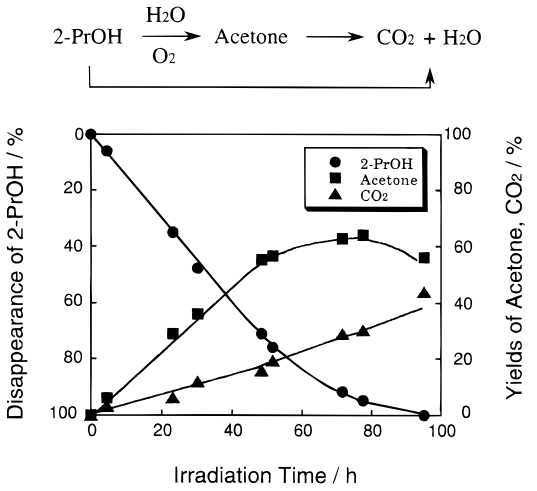

Figure 2. Reaction time profiles for the liquid-phase photocatalytic oxidative degradation of 2-propanol diluted in water to form acetone and CO_2 on the anchored titanium oxide/PVG catalyst (Ti content 4.3×10^{-7} mol/cat-g, ion acceleration energy 100 keV) prepared by the metal ion-implantation method.

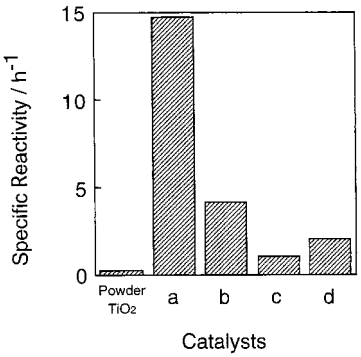

Figure 3. Specific photocatalytic reactivity for the oxidative degradation of 2-propanol on TiO_2 powder (P-25) and the anchored titanium oxide/PVG (a−d) catalysts prepared by the metal ion-implantation method. Amount of implanted Ti ions: (a) 4.3 ± 10^{-7}, (b) 8.7×10^{-7}, (c) 17.3×10^{-7}, (d) 4.3×10^{-7} mol/cat-g. Ion acceleration energy: (a−c) 100 keV; (d) 30 keV.

The specific photocatalytic reactivities for the initial degradation of 2-propanol are shown in Figure 3. The photocatalytic reactivities of these anchored titanium oxide/PVG catalysts prepared by advanced metal ion implantation were found to be much higher than that of an efficient standard photocatalyst of TiO_2 (P-25) particles. The specific photocatalytic reactivities of the anchored titanium oxide/PVG catalysts were remarkably enhanced in the regions of lower Ti content. The apparent quantum yields of the photocatalytic degradation of 2-propanol using these anchored titanium oxide/PVG catalysts implanted with Ti ions of 17.3×10^{-7}, 8.7×10^{-7}, and 4.3×10^{-7} mol/cat-g were 11%, 25%, and 93%, respectively. These values were much higher than the value of 9% with respect to the powdered TiO_2 photocatalyst. Titanium oxide/PVG photocatalysts are highly effective for liquid-phase reactions, and also the application of metal ion implantation used here is one of useful and promising procedures to prepare highly active photocatalysts on transparent glass plates. Furthermore, the quantum yields decreased with an increase in the content of the implanted Ti ions. Since the dispersion state and local structure of the Ti species in the catalyst depend greatly on the Ti content, as mentioned below, the photocatalytic reactivity is significantly affected by these structural changes.

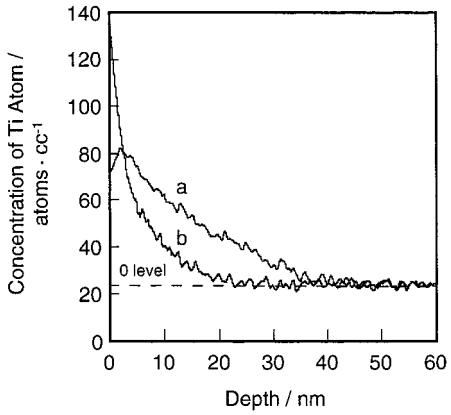

Figure 4. Depth profiles of Ti ions obtained by the analysis of the SIMS data with the anchored titanium oxide/PVG catalysts prepared by an advanced metal ion-implantation method: (a) Ti content 4.3×10^{-7} mol/cat-g, ion acceleration energy 100 keV; (b) Ti content 4.3×10^{-7} mol/cat-g, ion acceleration energy 30 keV.

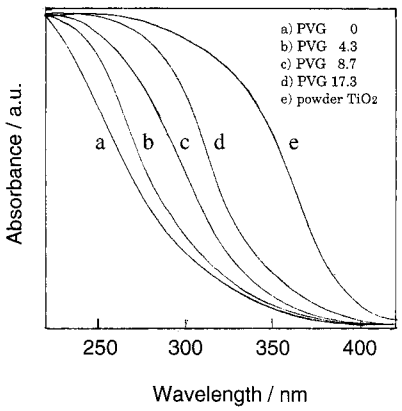

Figure 5. Absorption spectra of PVG (a), the anchored titanium oxide/PVG catalysts prepared by an advanced metal ion-implantation method (b−d), and TiO_2 powder (P-25) (e). Amount of implanted Ti ions: (b) 4.3×10^{-7}, (c) 8.7×10^{-7}, (d) 17.3×10^{-7} mol/cat-g. Ion acceleration energy: (b−d) 100 keV.

As shown in Figure 2, the CO_2 evolution in the oxidative degradation of 2-propanol can be observed along with the formation of acetone. This initial CO_2 evolution and the large quantum yields obtained with the anchored titanium oxide/PVG catalyst (93%) suggest that oxidative degradation proceeds with the chain reaction of organic radicals formed by the reaction with 2-propanol and the generated ·OH radicals.[14−16] In the presence of O_2, these ·OH radicals were formed in the following two types of reactions:

$$TiO_2 \rightarrow h^+ + e^-$$

$$e^- + O_2 \rightarrow O_2^-$$

$$O_2^- + 2H^+ + e^- \rightarrow H_2O_2$$

$$H_2O_2 + O_2^- \rightarrow \cdot OH + OH^- + O_2 \quad (1)$$

$$h^+ + H_2O \rightarrow \cdot OH + H^+ \quad (2)$$

Figure 3 also shows the photocatalytic reactivity of the catalyst prepared at a low acceleration energy of 30 keV. The reactivity of the catalyst prepared at 30 keV was less than that of the catalyst prepared at 100 keV, thus indicating that the high acceleration energy is significant in forming the active titanium oxide species.

The SIMS spectra were measured to evaluate the degree of the dispersion of the Ti ions on the silica glass plates. As shown in Figure 4a, the depth profiles of the Ti ions in the anchored titanium oxide/PVG catalysts prepared by Ti ion implantation at an acceleration energy of 100 keV showed that the Ti ions are mainly implanted within the region from the surface to the near surface layers of the silica glass plates at depths of about 40 nm. Decreasing the acceleration energy led to the implantation of a greater amount of Ti ions onto the top of the surface layer with a catalyst prepared at 30 keV (see Figure 4b).

The surface texture of the silica glass before and after Ti ion implantation was monitored by SEM analysis. There was no remarkable difference between the SEM images of the original porous silica glass and the Ti ion-implanted silica glass (17.3×10^{-7} Ti-mol/cat-g) prepared at 100 keV for 2 h. Also, no damage could be observed on the catalysts including smaller amounts of Ti ions (4.3×10^{-7} and 8.7×10^{-7} Ti-mol/cat-g). Furthermore, there was no difference in BET surface area between the unimplanted silica glass (250 m^2/g) and Ti ion-implanted silica glass. This ion-implantation technique caused no serious damages to the porous structure of the silica glass.

The absorption spectra of the anchored titanium oxide/PVG catalysts and the TiO_2 powdered catalyst recorded with a UV−vis diffuse reflectance spectrophotometer are shown in Figure 5. The anchored titanium oxide/PVG catalysts exhibited absorption bands in the wavelength regions 230−330 nm, shifting into shorter wavelength regions in comparison with the bulk TiO_2 catalyst at 390 nm. Such a shift of the absorption band to shorter wavelengths can be attributed to the size quantization effect which is in turn due to the presence of extremely small titanium oxide particles and/or the presence of highly unsaturated titanium oxide species having a tetrahedral coordination.[17−19] In fact, no XRD patterns with the anchored titanium oxide/PVG catalysts can be observed, indicating that the titanium oxide species anchored on PVG are highly dispersed and do not aggregate as titanium oxide crystals. A significant shift of the absorption band to shorter wavelengths can be observed with the anchored titanium oxide/PVG catalysts with low Ti content, clearly suggesting that the dispersion of the titanium oxide species on these catalysts is higher than that on catalysts prepared by conventional impregnation. A close relationship can thus be seen between the photocatalytic reactivity for the oxidative degradation of 2-propanol and the magnitude of the absorption shift toward shorter wavelength regions in these catalysts.

The Ti(2p) photoelectron transition for the anchored titanium oxide/PVG catalysts was measured by XPS spectroscopy, and the spectra obtained with the catalysts prepared at various acceleration energies are shown in Figure 6. The binding energies of Ti($2p_{3/2}$) bands in the XPS spectra of the anchored titanium oxide/PVG catalysts prepared at 70−100 keV were within the range of 459.3−459.8 eV, while that of powdered TiO_2 exhibited a band at 458.3 eV. The binding energies of the bands with these anchored titanium oxide/PVG catalysts were similar to those observed previously with the tetrahedral titanium oxide species in the titanium silicalite zeolites,[20−22] indicating that titanium oxides in tetrahedral coordination are present on the anchored titanium oxide/PVG catalysts. The larger shift in the band observed with titanium oxide/PVG is associated with the differential charge-up property of the tetrahedral titanium oxide species and strongly depends on the spatial distribution of the Ti species.

Figure 7 shows the surface Ti composition of the titanium oxide/PVG catalysts calculated from the ratio of the Ti($2p_{3/2}$) to Si($2p_{1/2}$) XPS band intensities. The decrease of acceleration

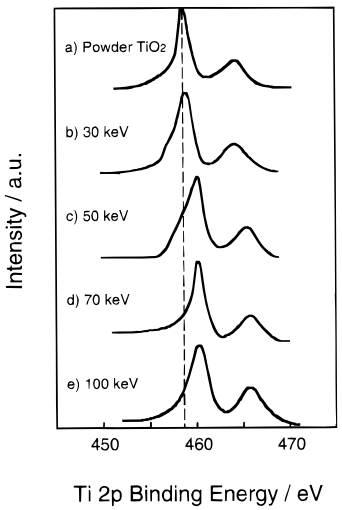

Figure 6. X-ray photoelectron spectra of the Ti 2p levels for TiO_2 powder (P-25) (a), the anchored titanium oxide/PVG catalysts prepared by an advanced metal ion-implantation method (b−e), and PVG (f). Ion acceleration energy: (b) 30, (c) 50, (d) 70, (e) 100 keV. Amount of implanted Ti ions: (b−e) 4.3×10^{-7} mol/cat-g.

energy for ion implantation obviously causes a steady increase of Ti composition on the surface. The bands shift to a lower binding energy with a decrease in the acceleration energy, and the catalyst prepared at 30 keV exhibits a band at 458.5 eV, similar to that of observed with TiO_2 powder (see Figure 6). From the relationship between the binding energy and Ti composition on the surface, the spatial distribution of the Ti species decreases with decreasing acceleration energy and the Ti species tend to aggregate on the top surface of the catalyst. This aggregation of the Ti species results in a decrease of the photocatalytic reactivity, as shown in Figure 3.

Figure 8 shows the XANES spectra of the anchored titanium oxide/PVG catalysts and the TiO_2 powdered catalyst. The XANES spectra of the titanium oxide catalysts at the Ti K-edge show several well-defined preedge peaks which are related to the local structures surrounding the Ti atom. The relative intensities of these preedge peaks provide useful information on the coordination number of the Ti atom.[20−23] The anchored Ti-oxide/PVG catalyst with lower Ti content exhibits an intense single preedge peak, as shown in Figure 8a. Since tetrahedrally coordinated Ti such as in $Ti(OPr^i)_4$ was found to exhibit an intense single preedge peak due to the lack of an inversion center in the regular tetrahedron structure, the observation of this intense single preedge peak clearly indicates that the titanium oxide species in the anchored titanium oxide/PVG catalyst exist in a tetrahedral coordination.

Figure 8 also shows the Fourier transforms of the EXAFS (FT-EXAFS) spectra of the catalysts, and all data are given without corrections for phase shifts. All of the catalysts investigated in the present study exhibit a strong peak around 1.6 Å which can be assigned to the neighboring oxygen atoms (Ti−O). The anchored titanium oxide/PVG catalyst with lower Ti content exhibits only Ti−O peaks, indicating the presence of isolated titanium oxide species on these catalysts. The curve-fitting analysis of the EXAFS spectra reveal that the anchored titanium oxide/PVG catalyst (4.3×10^{-7} mol/cat-g) consists of 4-coordinate titanium ions with a coordination number of 3.7 and an atomic distance of 1.81 Å. Increasing the Ti content in the anchored titanium oxide/PVG catalysts leads to a weakening of the preedge peak in the XANES spectra while other peaks attributed to the neighboring titanium atoms (Ti−O−Ti) appear in the FT-EXAFS spectra.

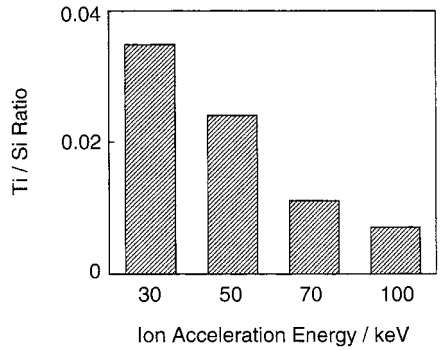

Figure 7. Surface composition of Ti calculated from the signal intensity of $Ti(2p_{3/2})$ and $Si(2p_{1/2})$ XPS bands observed for the anchored titanium oxide/PVG catalysts prepared by various ion acceleration energies (30−100 keV). Amount of implanted Ti ions: 4.3×10^{-7} mol/cat-g.

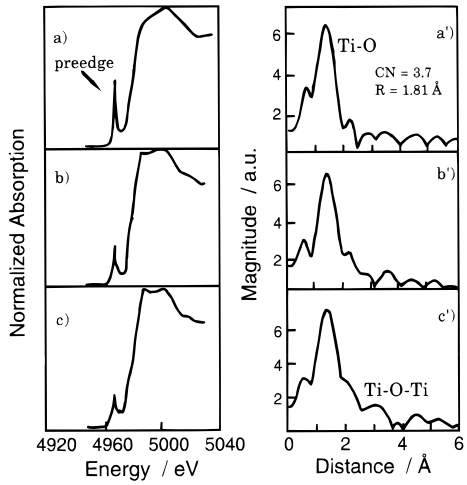

Figure 8. XANES (a−c) and FT-EXAFS (a′−c′) spectra of the anchored titanium oxide/PVG catalysts prepared by advanced metal ion implantation. Amount of implanted Ti ions: (a, a′) 4.3×10^{-7}, (b, b′) 8.7×10^{-7}, (c, c′) 17.3×10^{-7} mol/cat-g. Ion acceleration energy: 100 keV.

From XANES, FT-EXAFS, XPS, and UV−vis absorption spectral analyses, the calcinating titanium ions implanted onto porous silica glass are present as isolated titanium oxide moieties in a tetrahedral coordination and an increase in the Ti content or a decrease in the acceleration energy leads to the aggregation of the isolated titanium species, while the TiO_2 powdered catalyst involves an aggregated octahedral titanium oxide species.

The observed XAFS and UV−vis absorption spectra are in good agreement with those of the highly dispersed tetrahedrally coordinated titanium oxides anchored onto Vycor glass prepared by the CVD method with $TiCl_4$, where the absorption of UV light around 280 nm brings about an electron transfer from the lattice oxygen (O_l^{2-}) to the titanium ion (Ti_l^{4+}) to form a charge-transfer excited state.[1,7] It can thus be easily concluded that the observed efficient photocatalytic reactivity of the anchored titanium oxide species prepared by advanced metal ion implantation is attributed to the formation of the charge-transfer excited state of the highly distributed titanium oxide species having a tetrahedral coordination under UV irradiation.

Conclusions

Titanium oxide catalysts highly dispersed onto porous silica glass plates prepared by metal ion implantation exhibit high photocatalytic reactivity for the liquid-phase mineralization of 2-propanol to CO_2 and H_2O. Furthermore, the filtration of the

anchored photocatalysts from the liquid reactants was much easier than the fine TiO_2 particle dispersion. The calcinating titanium ions implanted onto the porous silica glass plate are present on the surface layer of the silica glass as isolated tetrahedral titanium oxide moieties which are found to be responsible for the high photocatalytic reactivity. Consequently, the titanium oxide catalysts dispersed onto porous silica glass are effective photocatalysts for liquid-phase reactions and advanced metal ion implantation is one of the useful and promising methods for the preparation of highly active photocatalysts.

Acknowledgment. This work was supported in part by Grants-in-Aid on the Priority Areas of Research on "Catalytic Chemistry of Unique Reaction Fields" (08232271), "Electrochemistry of Ordered Interfaces" (10131261), and "Carbon Alloys" (10137240) from the Ministry of Education, Science, Sports, and Culture of Japan.

References and Notes

(1) Anpo, M.; Yamashita, H. In *Surface Photochemistry*; Anpo, M., Ed.; John Wiley & Sons: Chichester, U.K., 1996; 117.
(2) Anpo, M. *Catal. Surv. Jpn.* **1997**, *1*, 169.
(3) Anpo, M.; Yamashita, H. In *Heterogeneous Photocatalysis*; Schiavello, M., Ed.; John Wiley & Sons: Chichester, U.K., 1997; 133.
(4) Fox, M. A.; Dulay, M. T. *Chem. Rev.* **1993**, *93*, 341.
(5) *Photocatalytic Purification and Treatment of Water and Air*; Ollis, D. F., Al-Ekabi, H., Eds.; Elsevier: Amsterdam, 1993.
(6) Anpo, M.; Yamashita, H.; Ichihashi, Y.; Fujii, Y.; Honda, M. *J. Phys. Chem. B* **1997**, *101*, 2632.
(7) Anpo, M.; Yamashita, H.; Ichihashi, Y.; Ehara, S. *J. Electroanal. Chem.* **1995**, *396*, 21.
(8) Yamashita, H.; Ichihashi, Y.; Harada, M.; Stewart, G.; Fox, M. A.; Anpo, M. *J. Catal.* **1996**, *158*, 97.
(9) Yamashita, H.; Kawasaki, S.; Ichihashi, Y.; Harada, M.; Takeuchi, M.; Anpo, M.; Stewart, G.; Fox, M. A.; Louis, C.; Che, M. *J. Phys. Chem. B* **1998**, *102*, 5870.
(10) Heller, A. *Acc. Chem. Res.* **1995**, *28*, 503.
(11) Anpo, M.; Ichihashi, Y.; Takeuchi, M.; Yamashita, H. *Res. Chem. Intermed.* **1998**, *24*, 143.
(12) Morin, B.; Davidson, D.; Che, M.; Ichihashi, Y.; Yamashita, H.; Anpo, M. *J. Phys. Chem. B*, in press.
(13) Yamashita, H.; Matsuoka, M.; Tsuji, K.; Shioya, Y.; Anpo, M.; Che, M. *J. Phys. Chem.* **1996**, *100*, 397.
(14) Serpone, N.; Lawless, D.; Khairutdinov, R.; Pelizzetti, E. *J. Phys. Chem.* **1995**, *99*, 16655.
(15) Schwitzgebel, J.; Ekerdt, J. G.; Gerischer, H.; Heller, A. *J. Phys. Chem.* **1995**, *99*, 5633.
(16) Turich, C. S.; Ollis, D. F. *J. Catal.* **1990**, *122*, 178.
(17) Anpo, M.; Nakaya, H.; Kodama, S.; Kubokawa, Y.; Domen, K.; Onishi, T. *J. Phys. Chem.* **1985**, *90*, 1633.
(18) Liu, X.; Iu, K.; Thomas, J. K. *J. Chem. Soc., Faraday Trans.* **1993**, *89*, 1861.
(19) Liu, Z.; Davis, R. J. *J. Phys. Chem.* **1994**, *98*, 1253.
(20) Bordiga, S.; Coluccia, S.; Lamberti, C.; Marchese, L.; Zecchina, A.; Boscherini, F.; Buffa, F.; Genoni, F.; Leofanti, G.; Petrini, G.; Vlaic, G. *J. Phys. Chem.* **1994**, *98*, 1253.
(21) Bonneviot, L.; On, D. T.; Lopez, A. *J. Chem. Soc., Chem. Commun.* **1993**, 685.
(22) Yamashita, H.; Ichihashi, Y.; Anpo, M.; Hashimoto, M.; Louis, C.; Che, M. *J. Phys. Chem.* **1996**, *100*, 16041.
(23) Davis, R. J.; Liu, Z. *Chem. Mater.* **1997**, *9*, 2311.